Available online at www.sciencedirect.com
SCIENCE DIRECT®
C. R. Chimie 8 (2005) 1067–1075
COMPTES RENDUS CHIMIE
http://france.elsevier.com/direct/CRAS2C/

Fullpaper / Mémoire

Mono- and bis-templated cyclic polyoxothiomolybdates with succinate and fumarate ions

Sébastien Floquet, Jérôme Marrot, Emmanuel Cadot *

Institut Lavoisier IREM, UMR 8637, université de Versailles, 45, avenue des États-Unis, 78035 Versailles, France

Received 15 July 2004; accepted after revision 23 September 2004

Available online 26 January 2005

Dedicated to Professor Francis Sécheresse on the occasion of his 60th birthday

Abstract

The action of succinate and fumarate ions as template on the self-condensation of the $\{Mo_2O_2S_2\}$ building block led to the bis-templated ring $[Mo_{12}O_{12}S_{12}(OH)_{12}(C_4H_4O_4)_2]^{4-}$ (**1**) (noted $[Mo_{12}\text{-succ}_2]^{4-}$) and the mono-templated ring $[Mo_{12}O_{12}S_{12}(OH)_{12}(OH_2)_4(C_4H_2O_4)]^{2-}$ (**2**) (noted $[Mo_{12}\text{-fum}]^{2-}$), respectively. Compounds **1** and **2** have been isolated as rubidium salt and structurally characterized by single crystal X-ray diffraction study. Both the compounds have been characterized in solution by ^{1}H NMR, in D_2O. Such a study reveals that a dynamic exchange exists for **1**, involving successive transfers of a succinate ion through the open-cavity delimited by the Mo_{12}-ring. Thermodynamic data for such successive exchange are given. Nevertheless, variable temperature ^{1}H NMR experiments in CD_3CN for **1** and **2** show that no conformational change has been detected between 303 and 227 K for the alkyl chain of the central fumarate and succinate ions. A short discussion was begun upon the structural relationships between the size of the alkyl chain and the nuclearity of the inorganic host. ***To cite this article: S. Floquet et al., C. R. Chimie 8 (2005)***

Résumé

Polyoxothiomolybdates cycliques construits par effet template autour d'ions succinate et fumarate. L'action des ions succinate et fumarate sur la polycondensation de l'unité $\{Mo_2O_2S_2\}$ conduit à la formation des composés cycliques $[Mo_{12}O_{12}S_{12}(OH)_{12}(H_4C_4O_4)_2]^{4-}$ (**1**) (noté $[Mo_{12}\text{-succ}_2]^{4-}$) et $[Mo_{12}O_{12}S_{12}(OH)_{12}(OH_2)_4(H_2C_4O_4)]^{2-}$ (**2**) (noté $[Mo_{12}\text{-fum}]^{2-}$), contenant respectivement deux ions succinate et un ion fumarate, logés au sein d'une cavité dont le périmètre est délimité par six fragments $\{Mo_2O_2S_2\}$. Ces deux cycles moléculaires ont été caractérisés structuralement à l'état solide par la diffraction des rayons X sur monocristal. Une étude par RMN du proton dans D_2O montre que les ions succinate contenu dans la cavité de **1** sont échangeables, alors que pour **2**, l'ion fumarate central est solidement ancré à l'intérieur du cycle. Une étude à température variable entre 275 et 310 K dans D_2O a permis de dégager les grandeurs de réaction $\Delta_r H°$ et $\Delta_r S°$ des deux réactions successives d'échange des ions succinate dans le cycle $[Mo_{12}]$. Par ailleurs, une étude à température variable dans l'acétonitrile entre 303 et 227 K montre que, d'une part, les processus d'échange observés dans D_2O sont totalement inhibés et d'autre part, pour **1** et **2**,

* Corresponding author.
E-mail address: cadot@chimie.uvsq.fr (E. Cadot).

1631-0748/$ - see front matter © 2005 Académie des sciences. Published by Elsevier SAS. All rights reserved.
doi:10.1016/j.crci.2004.09.015

l'ion « template » adopte une unique conformation, figée pour toute la gamme de températures étudiées. Enfin, ces deux nouveaux composés complètent une famille de cycles inorganiques, maintenant suffisamment fournie pour engager une discussion sur les relations entre la longueur de la chaîne alkyle de l'ion dicarboxylate et la nucléarité du cycle. ***Pour citer cet article : S. Floquet et al., C. R. Chimie 8 (2005)***

Keywords: Polyoxometalate; Molybdenum; Sulfur; Template effect

Mots clés : Polyoxométallate ; Molybdene ; Soufre ; Effet Template

1. Introduction

The design of clusters containing a large number of metal centers represents an intellectually stimulating challenge for the chemist since the nano-scale chemistry are situated at the boundary of molecular and condensed matter and envelops diverse fields such as biochemical processes, [1] catalysis [2–4] and material science [5,6]. In this context, cyclic transition metal clusters based on the $\{M_2S_2O_2\}$ building block constitute a fascinating emerging class of compounds [7]. The cyclic architecture of the cluster delimits a central cavity which presents a significant cationic character at the origin of striking properties related with supramolecular [8] and host–guest chemistry [9,10]. Anionic reagents such as phosphate or dicarboxylate ions have been inserted in the cavity by replacing the water molecules which initially line the cavity [11]. The substitution leads to size-controlled molecular wheels, more or less distorted and containing from eight [12] to 16 [13] metallic atoms. NMR studies in solution have revealed that strong dynamic synergistic effects between the guest and the host exist, reflecting the high flexibility of the hybrid architecture [14]. In a continuing project, we systematically investigate the host–guest interactions in such hybrid molecular materials, the goal being the understanding of the rules which govern the adaptability, the flexibility, the dynamic and the exchange properties of the encapsulated templates [15], because such compounds could be used for the inclusion of specific anionic substrates for transport or extraction processes. Herein, we report on the synthesis, the structural characterization and the behavior in solution of two cyclic hybrid molecular compounds $[Mo_{12}S_{12}O_{12}(OH)_{12}(C_4H_4O_4)_2]^{4-}$ (**1**, noted $[Mo_{12}\text{-}succ_2]^{4-}$) and $[Mo_{12}S_{12}O_{12}(OH)_{12}(H_2O)_4(C_4H_2O_4)]^{2-}$ (**2**, noted $[Mo_{12}\text{-fum}]^{2-}$), which consist of a Mo_{12}-ring templated by a four carbon linear dicarboxylate ion, i.e. fumarate and succinate ions, respectively.

2. Experimental

2.1. Synthesis

2.1.1. $Rb_3(NMe_4)[Mo_{12}\text{-}succ_2]\cdot 25\ H_2O$ (*1*)

The crude precursor $K_2I_2Mo_{10}S_{10}O_{10}(OH)_{10}(H_2O)_5]\cdot 15\ H_2O\cdot\varepsilon\ NMe_4I$ [11] (1 g; 0.41 mmol) was dissolved in 80 ml of water at 50 °C. Succinic acid (0.1 g; 0.8 mmol) was dissolved in 10 ml of water, basified by 1.6 ml of 1 mol l^{-1} KOH solution. The resultant potassium succinate solution was added to the previous one for giving an orange solution (about pH 5). The mixture was kept at 50 °C for 45 min and rubidium chloride (2.15 g; 17.7 mmol) is added. A yellow cloudy precipitate was removed by filtration and the resulting filtrate allowed to stand in air for crystallization. After several days, orange crystals suitable for X-ray diffraction are obtained, washed by water and dried in air. Yield 42%. Anal. Calc. (found) for **1**: Mo 39.09 (39.53), S 13.06 (12.90). EDX atomic ratio calcd. (found): Mo/S, 1 (0.98); Mo/Rb, 4 (3.90); S/Rb, 4 (3.96). IR/cm^{-1} (KBr pellet):1543(s), 1484(m), 1453(m), 1398(m), 939(s), 496(s), NMR ^1H in DMSO-d_6 per ppm: –0.70, 2.30, 3.04, 10.34.

2.1.2. $Rb_{1,5}K_{0.5}[Mo_{12}\text{-fum}]\cdot 19\ H_2O$ (*2*)

The crude precursor $K_2I_2Mo_{10}S_{10}O_{10}(OH)_{10}(H_2O)_5]\cdot 15\ H_2O\cdot\varepsilon\ NMe_4I$ [11] (1 g; 0.41 mmol) was dissolved in 60 ml of water at 50 °C. Fumaric acid (0.076 g; 0.60 mmol) was dissolved in 10 ml of water and 1.2 ml of 1 mol l^{-1} KOH solution. The resulting solution was added to the previous solution for giving a clear orange solution at pH about 4.5. A first fraction of the target compound was obtained by the addition of

RbCl (0.205 g; 1.7 mmol) to the solution (yield 32%). Single crystals suitable for the X-ray diffraction study were obtained from the filtrate which was allowed to stand for 1 week (yield 30%). Anal. Calc. (found) for **1**: Rb 4.91 (4.79), K 0.75 (0.85) Mo 44.14 (44.63), S 14.75 (14.66), C 1.84 (2.23). EDX atomic ratio calcd. (found): Mo/S, 1 (1.13); Mo/Rb, 8 (7.97); S/Rb, 8 (8.3). IR/cm^{-1} (KBr pellet):1558(s), 1387(m), 962(m), 521(m). NMR ^{1}H in DMSO-d$_6$ per ppm: 2.99, 10.31, 3.04, 10.34.

2.1.3. $Li_4[Mo_{12}\text{–}succ_2]\cdot n\ H_2O$ and $Li_2[Mo_{12}\text{-}fum]\cdot n\ H_2O$

The two lithium salts were prepared from the corresponding potassium salt $K_4[Mo_{12}\text{–}succ_2]\cdot nH_2O$ and $K_2[Mo_{12}\text{-fum}]\cdot n\ H_2O$, previously dissolved in water (about 0.4 g in 30 ml of water). Each solution was passed through a cation exchanger resin in the Li^+ form (Dowex 50WX2). The resultant solutions were evaporated until dryness, and the purity of the lithium salt checked by routine methods (^{1}H NMR, IR, EDX).

The potassium salts of **1** and **2** were prepared as the procedures previously described for the rubidium salt (see below). Instead RbCl, potassium chloride (4 g; 53.6 mmol) was added for the precipitation of the corresponding potassium salts. The crystalline solids of **1** and **2**, as potassium salts have been characterized by routine methods (^{1}H NMR, IR, EDX).

2.2. Physical methods

Elemental analysis was performed by the 'Laboratoire central d'analyse du CNRS' (Solaize, France). Water content was determined by thermal gravimetric analysis (tga7, Perkin–Elmer).

Infrared spectra were recorded on an Magna 550 Nicolet spectrophotometer, using KBr pellet.

NMR measurements were performed on a Brüker Avance 300 spectrometer, operating at 300 MHz in 5 mm tubes. Chemical shifts were referenced to the external usual TMS standard. The variable temperature ^{1}H NMR studies were performed in CD_3CN solution, 0.1 mol l^{-1} of lithium salt, $Li_4[Mo_{12}\text{–}succ_2]\cdot n\ H_2O$ or $Li_2[Mo_{12}\text{-fum}]\cdot n\ H_2O$, respectively.

2.2.1. X-ray crystallography

A single crystal of **1** was mounted in a 0.3 mm diameter Lindeman tube while a single crystal of **2** was stabilized in liquid glycerin (paratone). Intensity data were collected at room temperature (298 K) for **1** and 100 K for **2** with a Brüker X8, Kappa CCD three-circle diffractometer equipped using the Mo Kα monochromatized wavelength ($\lambda = 0.71073$ Å). An empirical absorption correction was applied using the SADABS program based on the method of Blessing [16,17]. The structures were solved by direct methods and refined by full-matrix least-squares using the SHELX-TL package [18]. Crystallographic data for **1** and **2** are reported in Table 1, selected bond distances are given in Table 2. Some Rb^+ cations and some oxygen atoms of water molecules were found disordered. All the disordered atoms and water of crystallization were refined isotropically, the other atoms were refined anisotropically. Hydrogen atoms of the alkyl chains of the succinate and fumarate ions were located with geometrical restraints in the riding mode. Lattice water found by single crystal X-ray diffraction method slightly disagrees with those found by TGA method for **1** and **2** crystals. Such a difference is currently encountered for those ionic compounds: water molecules are often highly disordered and crystals decompose in air with loss of water.

2.2.2. Structure of the anions

In Figs. 1 and 2 are depicted the molecular structure of the $[Mo_{12}\text{-}succ_2]^{4-}$ (**1**) and $[Mo_{12}\text{-fum}]^{2-}$ (**2**) anions. Crystal data and selected bond distances are given in Tables 1 and 2, respectively. The two $[Mo_{12}\text{-fum}]^{2-}$ and $[Mo_{12}\text{-}succ_2]^{4-}$ molecular architectures consist of an inorganic cyclic neutral skeleton $\{Mo_{12}S_{12}O_{12}(OH)_{12}\}$, encapsulating two succinate ion for **1** and one fumarate ion for **2**, respectively. The inorganic wheel results from $\{Mo_2O_2S_2\}^{2+}$ connections through double hydroxo bridges, giving non-bonding MoLMo contacts (3.282(1)–3.383(1) Å) while sulfur atoms within the building blocks spans the MoLMo bonding contacts (2.821(1)–2.855(2) Å).

2.2.3. $[Mo_{12}S_{12}O_{12}(OH)_{12}(H_2O)_4(C_4H_4O_4)_2]^{4-}$ (*1*)

The Mo_{12}-inorganic wheel encapsulates two succinate ions which are symmetrically arranged in the open-cavity (see Fig. 1). The four carboxylato groups exhibit the same asymmetric binding mode, each group being opposite to a single $\{Mo_2O_2S_2\}$. The O6 oxygen atom exhibits only one bonding contact with the Mo1 atom, while the O7 atom bridges the Mo2 and Mo3 atoms.

Table 1
Crystal data for **1** and **2**

	1	**2**
Formula	$C_{12}H_{54}Mo_{12}NO_{43}Rb_3S_{12}$	$C_4H_{74}K_{0.50}Mo_{12}O_{58}Rb_{1.50}S_{12}$
M (g mol^{-1})	2734.39	2692.97
T (K)	298(2)	100(2)
Crystal size (mm)	0.32 × 0.16 × 0.16	0.26 × 0.16 × 0.06
Crystal system	Orthorhombic	Triclinic
Space group	*Immm*	$P\bar{1}$
a (Å)	18.6607(13)	9.203(2)
b (Å)	11.0184(6)	14.055(4)
c (Å)	21.4067(12)	16.272(4)
α (°)	90	106.15(1)
β (°)	90	97.91(1)
γ (°)	90	99.53(1)
V (Å^3)	4401.5(5)	1956.1(9)
Z	2	1
ρ_{calc} (g cm^{-3})	2.032	2.321
μ (Mo Kα) (cm^{-1})	3.648	3.222
λ (Mo Kα) (Å)	0.71073	0.71073
θ Range (°)	1.45–29.98	1.33–40.95
Data collected	25,847	64,747
Unique data	3490	24,788
Unique data $I > 2\sigma(I)$	2315	15,921
Number of parameters	128	424
$R(F)$[a]	0.0644	0.0372
$R_w(F^2)$[b]	0.0893	0.0749
Goodness-of-fit	1.092	1.026

[a] $R_1 = \dfrac{\Sigma \left|F_o\right| - \left|F_c\right|}{\Sigma \left|F_c\right|}$ [b] $R_w = \sqrt{\dfrac{\Sigma\, w\,(F_o^2 - F_c^2)^2}{\Sigma\, w\,(F_o^2)^2}}$ $\dfrac{1}{w} = \sigma^2 F_o^2 + (aP)^2 + bP$

The 12 molybdenum exhibit an octahedral arrangement and are arranged in a C_{2v} idealized local symmetry.

2.2.4. $[Mo_{12}S_{12}O_{12}(OH)_{12}(OH_2)_4(C_4H_2O_4)]^{2-}$ (**2**)

The structure reveals the presence of one encapsulated fumarate ion $[H_2C_4O_4]^{2-}$ in the Mo_{12}-ring (Fig. 2). The organic template is nearly located at the center of the elliptically distorted ring (C_{2h} idealized molecular symmetry) and connected through the two symmetric carboxylato groups. Four molybdenum atoms are involved in a bonding contact with the organic guest, while the coordination sphere of the other eight is filled by four inner water molecules (O14 and O15) which are doubly bonded to two adjacent molybdenum atoms. The carboxylato groups bridge two adjacent molybdenum atoms (Mo1 and Mo6), belonging to two different $\{Mo_2O_2S_2\}$. Such a mode of connection differs of those previously encountered, where the carboxylato groups are directly connected to the two adjacent molybdenum atom of the same $\{Mo_2O_2S_2\}$ unit [14]. Such a result is attributed to steric constraints induced by the rigidity of the central C=C double bond of the guest, which imposes the conformational arrangement of the inorganic host around the rigid template.

2.2.5. ^1H NMR in D_2O

Besides the signal of the solvent (presence of H_2O), the spectrum of $[Mo_{12}\text{-fum}]^{2-}$ (not shown) exhibits a sharp resonance at 3.02 ppm corresponding to the two equivalent protons attached to the encapsulated fumarate ion. The uncoordinated fumarate is observed at 6.4 ppm. The ^1H NMR spectrum of the $[Mo_{12}\text{-succ}_2]^{4-}$ (Fig. 3) reveals more complicated, since three resonances corresponding to three different environments for the succinate ions are observed. At 295 K, the broad peak at 2.2 ppm is attributed to the uncoordinated succinate ions, while the two shielded resonances at

Table 2
Selected bond lengths

For (**1**)		
Mo1	O1	1.710(6)
	O4	2.103(5)
	O4	2.103(5)
	S1	2.318(2)
	S1	2.318(2)
	O6	2.336(9)
	Mo2	2.821(1)
	Mo1	3.385(1)
Mo2	O2	1.694(9)
	O5	2.101(5)
	O5	2.101(5)
	S1	2.325(2)
	S1	2.325(2)
	O7	2.325(7)
	Mo1	2.821(1)
	Mo3	3.281(1)
Mo3	O3	1.687(8)
	O5	2.088(4)
	O5	2.088(4)
	S2	2.323(2)
	S2	2.323(2)
	O7	2.579(7)
	Mo3	2.841(1)
	Mo2	3.281(1)
C1	O7	1.225(2)
	O6	1.262(2)
	C2	1.597(2)
C2	C2	1.483(2)
For (**2**)		
Mo1	O1	1.690(1)
	O7	2.099(1)
	O8	2.125(1)
	S1	2.323(1)
	S2	2.330(2)
	O13	2.345(1)
	Mo2	2.831(1)
	Mo6	3.383(1)
Mo2	O2	1.695(1)
	O10	2.096(2)
	O9	2.116(1)
	S2	2.318(1)
	S1	2.326(2)
	O14	2.541(2)
	Mo1	2.831(1)
	Mo3	3.329(2)
Mo3	O3	1.673(1)
	O10	2.085(1)
	O9	2.118(2)
	S3	2.315(1)
	S4	2.329(2)
	O14	2.645(1)
	Mo4	2.834(2)
	Mo2	3.329(2)
Mo4	O4	1.682(1)
	O11	2.067(1)
	O12	2.109(1)
	S3	2.325(2)
	S4	2.331(1)
	O15	2.606(1)
	Mo3	2.834(2)
	Mo5	3.316(1)
	O3	3.498(2)
Mo5	O5	1.683(1)
	O11	2.079(1)
	O12	2.100(1)
	S6	2.328(2)
	S5	2.332(1)
	O15	2.583(2)
	Mo6	2.855(2)
	Mo4	3.316(1)
Mo6	O6	1.690(1)
	O7	2.109(1)
	O8	2.136(2)
	O16	2.271(2)
	S5	2.325(1)
	S6	2.341(1)
	Mo5	2.855(2)
	Mo1	3.383(2)
C1	O13	1.262(1)
	O16	1.276(1)
	C2	1.494(1)
C2	C2	1.309(1)

–0.01 and –0.66 ppm correspond to encapsulated species. The presence of uncoordinated succinate ions reveals that succinate ion exchange occurs in the ring, and the simplest equilibrium (Eq. 1) can be postulated.

$$[Mo_{12}\text{-}Succ_2]^{4-} \rightleftharpoons [Mo_{12}\text{–succ}]^{2-} + succ^{2-} \quad (1)$$

The intensity and the broadness of the –0.01 ppm line should argues for its attribution to the mono-succinate species. At upper temperature than 300 K, this line (–0.01 ppm) and that at 2.2 ppm exhibits nearly

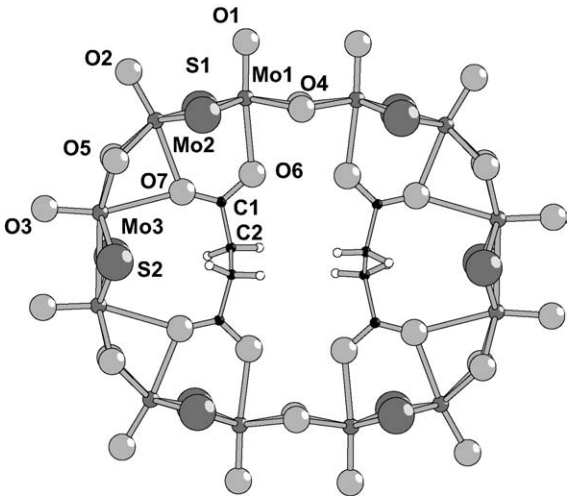

Fig. 1. Molecular structure of $[Mo_{12}S_{12}O_{12}(OH)_{12}(C_4H_4O_4)_2]^{4-}$ (**1**).

equal intensities according to the equilibrium 1, while the broadness of the –0.01 ppm line ($\Delta\nu_{1/2}$ = 50 Hz) would reflect the possibility of the remaining encapsulated succinate ion to move inside the half-empty cavity of Mo_{12}-ring. The remaining line at –0.66 ppm would be then attributed to the bis succinato-containing species $[Mo_{12}\text{-succ}_2]^{4-}$, involved in the equilibrium 1. In an aprotic solvent as CD_3CN, the equilibrium 1 reveals totally cancelled since only one line is observed at –0.65 ppm, corresponding to the bis succinato compound $[Mo_{12}\text{-succ}_2]^{4-}$. The decrease of the temperature from 310 to 275 K changes drastically the distribution in the species as shown by the variable temperature ^{1}H NMR experiments presented in Fig. 3. A second equilibrium (Eq. 2) must be considered necessarily, involving a second exchange process of the succinate ion from the mono-succinato compound $[Mo_{12}\text{-succ}]^{2-}$.

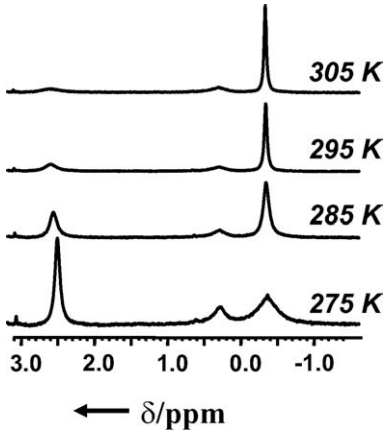

Fig. 3. Selected variable-temperature ^{1}H NMR spectra of $[Mo_{12}S_{12}O_{12}(OH)_{12}(C_4H_4O_4)_2]^{4-}$ (**1**) in D_2O.

$$[Mo_{12}\text{-Succ}]^{2-} \rightleftharpoons [Mo_{12}] + succ^{2-} \quad (2)$$

The equilibrium 2 gives an additional species, i.e. a templated-free Mo_{12}-ring, noted $[Mo_{12}]$. The concentration of overall species can be calculated from the initial concentration in $[Mo_{12}\text{-succ}_2]^{4-}$ (C = 3.85 × 10^{-3} mol l^{-1}), the intensities of the ^{1}H NMR lines, the mass balance in succinate and in Mo_{12}-species. The results are graphically shown in Fig. 4a and reveal that

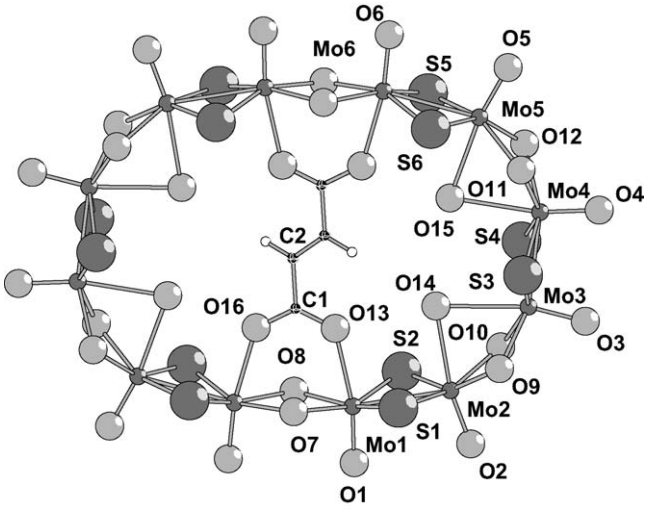

Fig. 2. Molecular structure of $[Mo_{12}S_{12}O_{12}(OH)_{12}(OH_2)_4(C_4H_2O_4)]^{2-}$ (**2**).

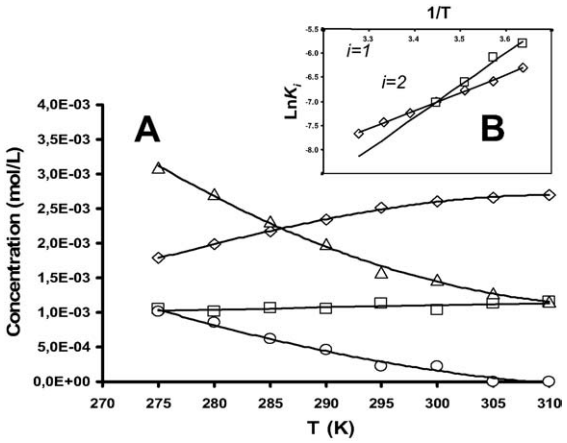

Fig. 4. (a) Variation of the distribution in $[Mo_{12}\text{-}succ_2]^{4-}$ (Δ), $[Mo_{12}\text{-}succ]^{2-}$ (□), $[Mo_{12}]$ (◇), $[succ]^{2-}$ (○) with temperature; (b) Van't Hoff linear plots $\ln K_i = f(1/T)$ with $i = 1, 2$.

as temperature decreases, the concentration in $[Mo_{12}\text{-}succ_2]^{4-}$ strongly decreases for giving uncoordinated succinate ions and succinate-free Mo_{12} compound. As a consequence of the successive equilibria, concentrations of the intermediary compound $[Mo_{12}\text{-}succ]^{2-}$ do not vary significantly. Then, the equilibrium constants K_1 and K_2 could be calculated in the 310–273 K temperature range, according to the Eqs. 3 and 4, respectively.

$$K_1 = \frac{[[Mo_{12}succ]^{2-}][succ]^{2-}]}{[[Mo_{12}succ_2]^{4-}]} \quad (3)$$

$$K_2 = \frac{[[Mo_{12}]][succ]^{2-}]}{[[Mo_{12}succ]^{2-}]} \quad (4)$$

Then, a Van't Hoff treatment of $\ln K_i$ ($i = 1, 2$) versus $1/T$ (shown in Fig. 4B) allowed to extract the standard enthalpy for the reactions 1 and 2; the standard entropy was then calculated from the Gibb's function. The calculated thermodynamic parameters for both successive succinate transfers are given in Table 3. The negative values found for enthalpy and entropy for Eqs. 1 and

Table 3
Thermodynamic parameters for the both successive succinate transfers from $[Mo_{12}\text{-}succ_2]^{4-}$

Eqs.	$\Delta_r H°$ (kJ mol^{-1})	$\Delta_r S°$ (J K^{-1} mol^{-1})
1	–29.1 ± 0.2	–158 ± 1
2	–55.7 ± 0.5	–251 ± 2

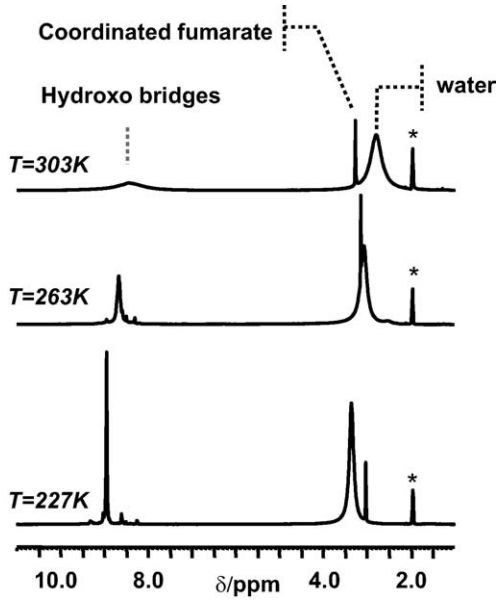

Fig. 5. Variable-temperature ^{1}H NMR of $[Mo_{12}S_{12}O_{12}(OH)_{12}(OH_2)_4(C_4H_2O_4)]^{2-}$ (**2**) as Li salt in CD_3CN. The peaks marked with an asterisk (*) correspond to the solvent (CHD_2CN).

2 could be tentatively attributed to the formation of the hydration sphere of the produced ionic species, i.e. the uncoordinated succinate ions. Such an interpretation would reflect the main contribution of the polar water molecules. In fact, the origin of the driving force governing the inclusion of the dicarboxylate within the cavity is the entropy increase.

2.2.6. Variable-temperature ^{1}H NMR in CD_3CN

The ^{1}H NMR spectra of $Li_4[Mo_{12}\text{-}succ_2]\cdot n\ H_2O$ is presented in Fig. 5. In CD_3CN, the spectra for both compounds, $Li_4[Mo_{12}\text{-}succ_2]\cdot n\ H_2O$ (not shown) and $Li_2[Mo_{12}\text{-}fum]\cdot n\ H_2O$ (Fig. 5) contain three types of signal related to the three types of protons present in the alkyl chain, in water and in the hydroxo bridges of the ring [14]. For both the compounds, at 303 K, the protons of the alkyl chain give one single sharp resonance at –0.54 and + 3.27 ppm for succinate and fumarate in Mo_{12}-ring, respectively. The deshielded domain exhibits one broad symmetric signal at about +9 ppm which corresponds to the hydroxo groups of the inorganic wheel. As the temperature decreases from 303 to 227 K, the signal of the hydroxo bridges remains single but sharpens drastically from about 50 to 5 Hz. Similarly, the peak of the water at 3.2 ppm exhibits the same type of behavior, revealing a dynamic exchange be-

tween protons of the rings and those of the water. Although those results cannot be entirely explained (only one signal for the hydroxo bridges is observed, instead of the two expected), they argues for a single host–guest conformation, likely due to impossibility of the substrate to wheel inside the cavity. In the $[Mo_{12}\text{-fum}]^{2-}$ anion, the rigidity of the linear chain probably cancels any concerted hopping of both the carboxylato groups, while in the $[Mo_{12}\text{-succ}_2]^{4-}$, the presence of two guests, closely arranged in the cavity prevents any conformational change of both the succinate ions.

3. Discussion

These results exemplify the potentialities of such a host–guest system and give two additional compounds in the series of the dicarboxylate templated rings. Relationships between the size of the inner linear chain and the nuclearity of the ring are evidenced and merit to be discussing herein. C2, C4, C5, C7 and C9 linear saturated chain of dicarboxylate ions have provide rings with variable nuclearity from eight to 16 with M=Mo and W. In this system, the templated rings are of two types, i) the mono-templated rings as $[Mo_{10}\text{-glu}]^{2-}$, $[Mo_{12}\text{-pim}]^{2-}$ [14], $[Mo_{14}\text{-aze}]^{2-}$ [19] and the bis-templated as $[Mo_{12}\text{-succ}_2]^{4-}$ and $[W_{16}\text{-glu}_2]^{4-}$ [13]. For the Mo series, the dependence of the nuclearity of a ring (y) with respect of the number of carbon atoms (x) in the alkyl chain is graphically shown in Fig. 6. The odd series with the C5, C7 and C9 chains gives exclusively the mono-templated Mo_{10}, Mo_{12} and Mo_{14} rings, respectively, and provides a linear correlation (a) ($y = x + 5$) presented in Fig. 6. With the succinate ion, a C4 even alkyl chain, the Mo8 is obviously too small for containing the C4 chain, while the C4 chain is expected also to be too small for a Mo_{10} ring, which perfectly matches with a C5 chain [14]. In this case, the expansion of the ring is observed for giving a bis-templated $[Mo_{12}\text{-succ}_2]^{4-}$. This observation could be extended for the prediction of few additional structures. For the previous reasons, the even C_6 and C_8 alkyl chains cannot give neither Mo_{10}, Mo_{12} nor Mo_{14} mono-templated rings. An expansion of the ring is then expected with such dicarboxylate ions for giving bis-templated arrangements. According to the equation (a), the increasing of two carbon in the chain provokes the increase of 2 Mo in the ring. For the bis-templated ring,

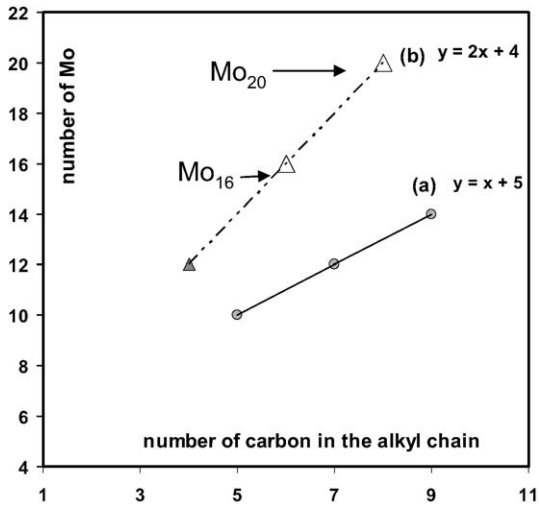

Fig. 6. Plots of the nuclearity of the Mo_{2n} ring versus the length of the alkyl chain: (**a**) odd series giving the mono-templated rings; (**b**) even series leading to the bis-templated rings, revealing two predicted compounds, the Mo_{16} and Mo_{20} rings.

the two carbon extension of both the C_{2n} chains should be accompanied by the expansion of 4 Mo, giving the (b) curve in Fig. 6. Finally, the bis-templated series could be described by the curve (b) in Fig. 6, giving the postulated Mo_{16} and Mo_{20} rings with C_6 and C_8 linear dicarboxylate ions, respectively. Recently, some preliminary results we obtained with C6 ion (elemental analysis) seem to confirm the formation of the bis-templated Mo_{16} ring. Studies are currently in hand to provide unambiguous characterizations for the Mo_{16} and Mo_{20} bis-templated rings.

4. Concluding remarks

This work presents two novel templated-Mo_{12}-rings with fumarate and succinate ions. Beside the structural characterizations, ^{1}H NMR studies in solution gave some fundamental insights about thermodynamic of the template exchange within the rings. Those results should be considered for the synthesis of more sophisticated hybrid molecular materials. Finally, some reasonable predictions can be made in the field of our own knowledges.

5. Supporting information available

Further details of the crystallographic data of **1** and **2** can be obtained from the Cambridge Crystallo-

graphic Data Center, 12 Union Road, Cambridge CB2 IEZ, UK (fax: +44-1223-33-6033 or e-mail: deposit@cdc.cam.ac.uk) as supplementary publication on quoting the depository number, No. CCDC-244995 for **1** and No. CCDC-244996 for **2**.

Acknowledgements

Ludovic Lecroq, M.Sci. student, is acknowledged for his contribution to the experimental work.

References

[1] J.T. Rhule, C.L. Hill, D.A. Judd, Chem. Rev. 98 (1998) 327–357.
[2] C.L. Hill, Polyoxometalates in catalysis, J. Mol. Catal. 114 (1996) 1–371.
[3] T. Okuhara, N. Mizuno, M. Misono, Adv. Catal. 41 (1996) 113–252.
[4] C.K. Loong, P. Thiyagarajan, J.W. Richardson, M. Ozawa, S. Susuki, J. Catal. 171 (1997) 498.
[5] D. Fenske, N. Zhu, T. Langetepe, Angew. Chem. Int. Ed. Engl. 37 (19) (1998) 2640–2643.
[6] L. Cronin, P. Kögerler, A. Müller, J. Solid-State Chem. 152 (2000) 57–67.
[7] F. Sécheresse, E. Cadot, A. Dolbecq, J. Solid-State Chem. 152 (2000) 78–86.
[8] E. Cadot, B. Salignac, J. Marrot, A. Dolbecq, F. Sécheresse, Chem. Commun. (2000) 261–262.
[9] E. Cadot, B. Salignac, T. Loiseau, A. Dolbecq, Chem. Eur. J. 5 (1999) 3390–3398.
[10] A. Dolbecq, E. Cadot, F. Sécheresse, C.R. Acad, Sci. Paris, Série IIc 3 (2000) 193–197.
[11] E. Cadot, B. Salignac, S. Halut, F. Sécheresse, Angew. Chem. Int. Ed. Engl. 37 (5) (1998) 611–612.
[12] A. Dolbecq, B. Salignac, E. Cadot, F. Sécheresse, Bull. Pol. Acad. Sci. 46 (1998) 237.
[13] E. Cadot, J. Marrot, F. Sécheresse, Angew. Chem. Int. Ed. Engl. 40 (2001) 774.
[14] B. Salignac, S. Riedel, A. Dolbecq, F. Sécheresse, E. Cadot, J. Am. Chem. Soc. 122 (2000) 10381–10389.
[15] E. Cadot, F. Sécheresse, Chem. Commun. (2002) 2189–2197.
[16] R. Blessing, Acta Crystallogr. Sect. A 51 (1995) 33.
[17] G.M. Sheldrick, a program for the Siemens Area Detector ABSorption correction, University of Göttingen, Germany, 1997.
[18] G.M. Sheldrick, SHELX-TL version 5.03, Software Package for the Crystal Structure Determination, Siemens Analytical X-ray Instruments Inc, Madison, WI, USA, 1994.
[19] S. Floquet, E. Cadot, J. Marrot, Unpublished results